ARTICLE

OBC
www.rsc.org/obc

Formation of gold-like metal-lustrous inclusion crystals from 1-phenyl-2,5-bis[5-(tricyanoethenyl)-2-thienyl]pyrrole host and an electron-donating aromatic guest

Katsuyuki Ogura,[*a,b] **Rui Zhao,**[b] **Takashi Mizuoka,**[a] **Motohiro Akazome**[a] **and Shoji Matsumoto**[a]

[a] *Department of Materials Technology, Faculty of Engineering, Chiba University, 1-33 Yayoicho, Inageku, Chiba 263-8522, Japan*
[b] *Graduate School of Science and Technology, Chiba University, 1-33 Yayoicho, Inageku, Chiba 263-8522, Japan*

Received 10th March 2003, Accepted 8th September 2003
First published as an Advance Article on the web 1st October 2003

A novel π-conjugated organic compound, 1-phenyl-2,5-bis[5-(tricyanoethenyl)-2-thienyl]pyrrole, which bears two powerful electron-withdrawing tricyanoethenyl substitutents, readily yielded gold-like metal-lustrous inclusion crystals with a series of aromatic guest molecules such as toluene, *p*-xylene, anisole, dimethoxybenzenes and indene. All the inclusion compounds have a common stoichiometric ratio (host/guest) of 2 : 1. X-Ray structural analyses demonstrate that the structural feature for toluene included crystal is similar to those containing *p*-xylene, anisole, dimethoxybenzenes and indene.

Introduction

Recently, we have reported that 1-aryl-(2-thienyl)-5-[5-(tricyanoethenyl)-2-thienyl]pyrroles **1**, a new class of π-conjugated compounds comprised of a stronger π-electron-withdrawing tricyanoethenyl substituent and a conjugated thiophene–pyrrole–thiophene skeleton, shows gold- or bronze-like metallic lusters.[1] The essential relationship between their vivid metallic colored appearance and their unique crystal structure, as well as the possibility of their applications in novel functional materials motivated us to explore this work more systematically and deeply. Hitherto, we have synthesized a large number of new compounds bearing one tricyanoethenyl group. By comparing their properties, we realised that the metal-like appearance is not exclusively limited to compound **1**, but is also possible with inclusion crystals containing **1** as the host molecule,[2] and the metallic colors are more diverse besides the predominant gold and bronze.[3] As a part of our investigation, we also synthesized the title compound **2** bearing two tricyanoethenyl groups, and found that crystallization of **2** from its DMF solution results in formation of bronze-like microcrystals with inclusion of DMF. Further studies have revealed that gold-like inclusion crystals can be formed by effective inclusion of **2** with various electron-donating aromatic molecules such as toluene, *p*-xylene, anisole, dimethoxybenzenes, and indene. Herein we report this inclusion phenomenon as well as the relationship between crystal appearance and crystal structure.

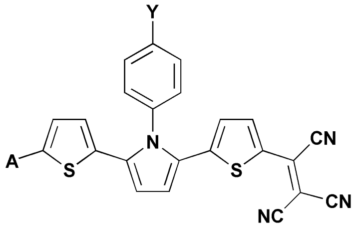

1: A = H;

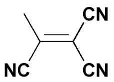

2: A = ; Y = H

Results and discussion

The host compound **2** was readily synthesized by treatment of its precursor, 1-phenyl-2,5-di(2-thienyl)pyrrole[1,4] with excess amount of tetracyanoethylene in DMF solution at 80 °C. After the reaction mixture cooled to room temperature, a large portion of the products precipitated as bronze-like microcrystals with inclusion of about 1.66 equivalents of DMF (determined by ^{1}H NMR spectrum and TG-DSC). The filtrate was concentrated to obtain the remaining portion. After chromatographic purification and then washing several times with acetone, **2** was obtained in a satisfactory yield (total 94%) and pure enough for further work.

Interestingly, after drying the DMF-included crystals *in vacuo* at 80–90 °C, a bright green powder, which was confirmed as pure **2**, was obtained. Upon exposure to DMF vapor in a closed vessel at room temperature for 24 h, the bright green powder returned again to the initial microcrystals with bronze-like metallic lustre. The X-ray powder diffraction (XRPD) patterns concerning the aforementioned changes clarify that the product from gas–solid reaction of **2** with DMF is similar to that prepared by crystallization, but is different from that of pure **2**, as shown in Fig. 1. This undoubtedly demonstrates

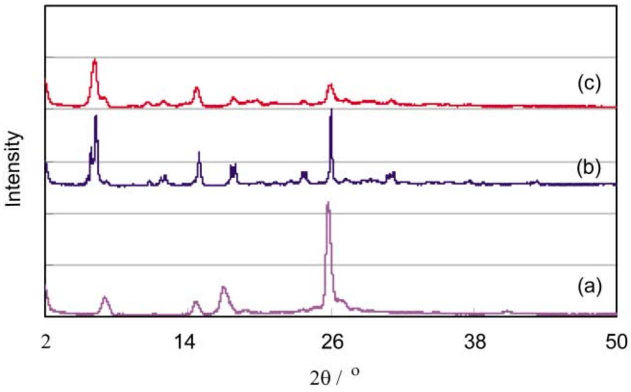

Fig. 1 Experimental XRPD traces of (a) pure host **2**, (b) crystals of complex **2**·DMF prepared by recrystallization and (c) crystals of complex **2**·DMF prepared by gas–solid reaction.

DOI: 10.1039/b302689b

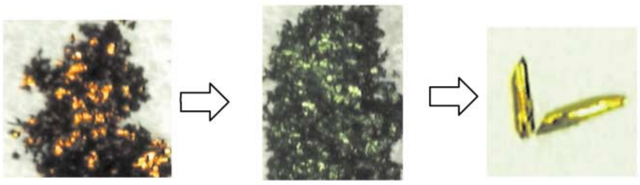

DMF included **2** (A) pure **2** only (B) toluene included **2** (C)

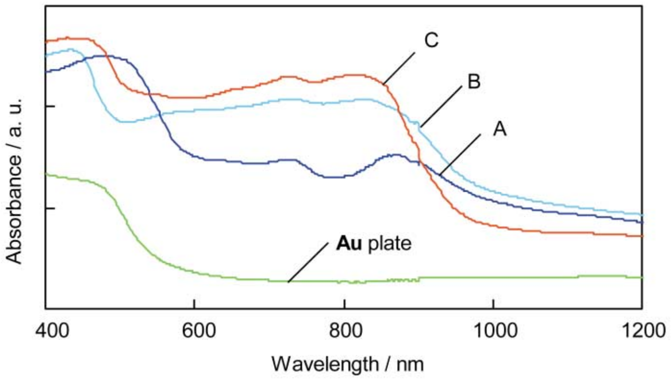

Fig. 2 Photographs (top) and solid-state UV-Vis-NIR diffuse absorption–reflection spectra (bottom) of the pure host **2** (curve B, λ_{max} = 440 nm) and its inclusion crystals with DMF (curve A, λ_{max} = 510 nm) and toluene (curve C, λ_{max} = 480 nm). For comparison, Au-plate is also shown as the bottom line (λ_{max} = 480 nm). Note that curve C resembles well with the Au-plate.

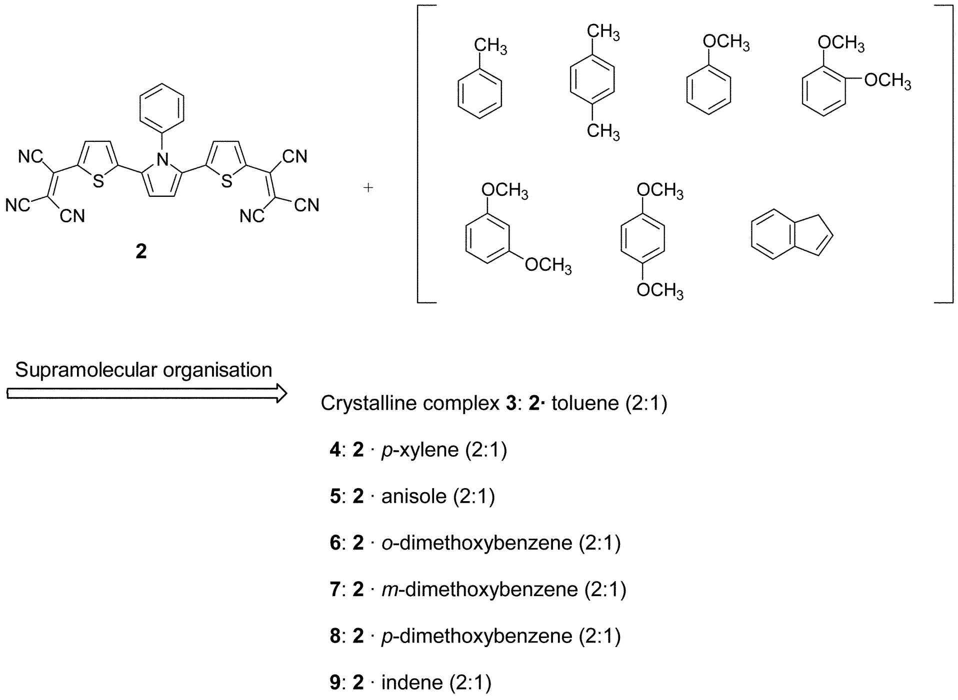

Scheme 1

that the DMF-included **2** is not a simple surface adsorption product, but a host–guest complex. To our surprise, gold-like single crystals of **2** suitable for X-ray analysis grew easily when toluene was employed as crystallization solvent. The interesting color change process is clearly reflected in the solid-state UV-Vis-NIR diffuse reflection–absorption spectra, shown in Fig. 2. The ^{1}H NMR spectrum shows that toluene (precisely 0.5 equivalent to **2**) is included in the crystals. X-Ray analysis also certifies that the single crystal is an inclusion compound of **2** and toluene with a stoichiometric ratio of 2 : 1. Other substituted benzenes such as *p*-xylene, anisole *etc*. were also examined for formation of inclusion crystals with **2**. The results are summarized in Scheme 1.

The following three simple procedures were used to obtain the inclusion crystals: i) Directly dissolving **2** into the respective guests and crystallising gradually from these produced solutions without the need for any other solvent when the guest is a volatile liquid at ambient temperature. Inclusion compounds **3**, **4**, and **5** were obtained in this way as gold-like metal-lustrous single crystals suitable for X-ray analysis and other measurements. ii) Dissolving the host–guest mixture into $CHCl_3$ solvent and crystallising by slow evaporation of the solvent when the guest is a liquid with a high boiling point (non-volatile) or a solid at ambient temperature. We attempted to prepare single crystals of the inclusion compounds **6**–**9** by this procedure and, with the exception of **6**, single crystals of **7**–**9** of a good quality suitable for X-ray analysis were obtained. Although **6** indisputably forms an inclusion compound with 2 : 1 host/guest ratio similar to that of **7**–**9** as determined by the ^{1}H NMR spectrum, X-ray analysis could not be achieved successfully because of the poor crystal quality. iii) Dissolving **2** in the non-volatile liquid guests and crystallising by slow diffusion of hexane into the host–guest mixtures. The inclusion compounds formed by this method, such as **6** and **7**, were always micro-crystals of poor quality unsuitable for X-ray analysis, but quite satisfactory for elemental analysis. The inclusion compounds **3**–**9** have a common stoichiometric ratio (host/guest) of 2 : 1. Crystallographic data are given in Table 1.†

Inclusion crystals **3**, **4**, and **5**, grown from the guest solution of the host **2**, are isostructural and crystallise with 4 host and 2 guest molecules in the monoclinic $P2_1/c$ space group. Inclusion crystals **8** and **9**, grown from the $CHCl_3$ solution of the host–guest mixture, are isostructural with **3**, **4** and **5**, and also crystallise with 4 host and 2 guest molecules in the monoclinic $P2_1/c$ space group. Crystal **7**, prepared similarly to **8** and **9**, has similar structure feature to the above-mentioned inclusion compounds, though it crystallises with 8 host and 4 guest molecules in the monoclinic $P2_1/c$ space group. For crystal **6**, although its X-ray analysis could not be achieved successfully because of its poor quality, we surmise that **6** is also virtually isostructural with **7**, as suggested by the XRPD patterns displayed in Fig. 3.

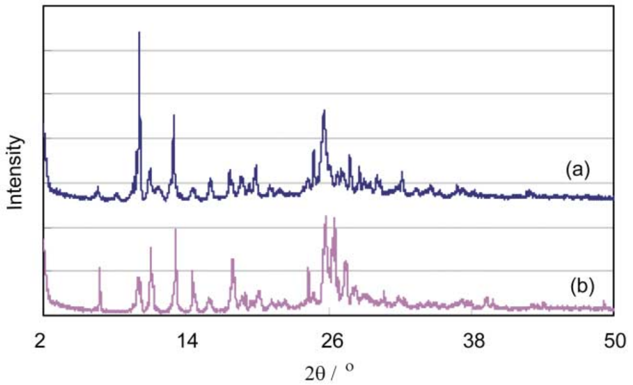

Fig. 3 Experimental XRPD traces of (a) inclusion crystals **6** and (b) **7**.

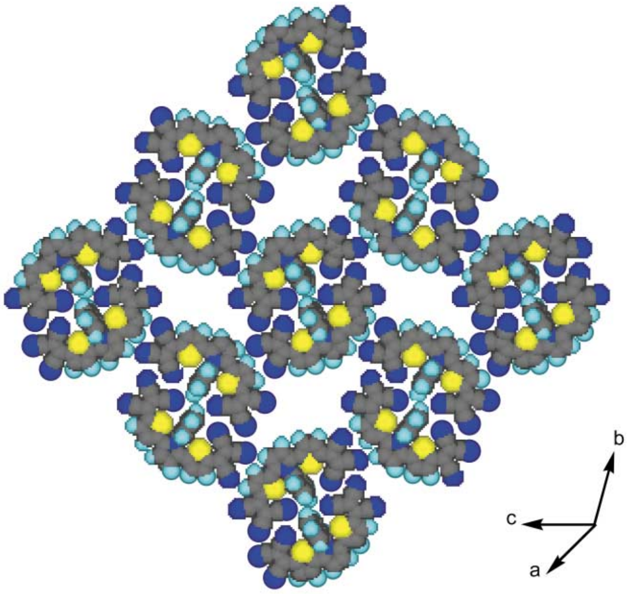

Fig. 4 Space-filling projection of inclusion crystal **3** viewed along the *a*-axis with guest molecules omitted, showing the open cavities.

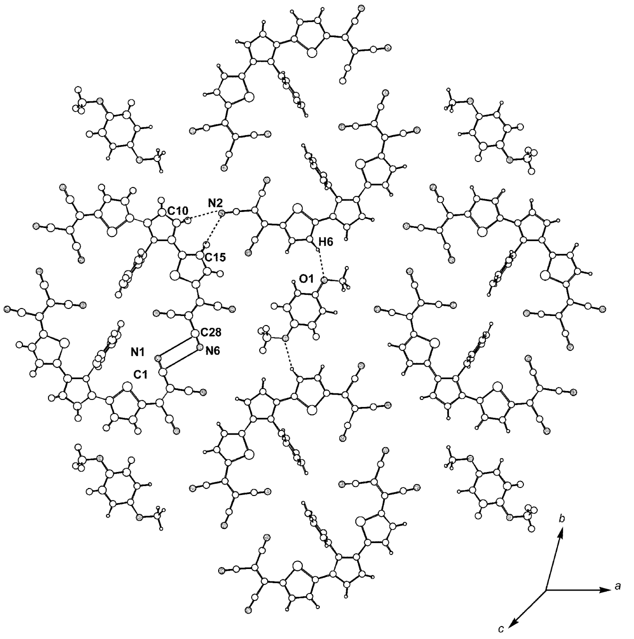

Fig. 5 Packing diagram of inclusion crystal **8** viewed along the *c*-axis. The CN ··· CN contacts (N1 ··· C28: 3.57 Å; N6 ··· C1: 3.59 Å) and the CH/N type hydrogen bonds [C10–H10 ··· N2: 2.65 Å (163.7°); C13–H13 ··· N2: 2.69 Å (171.3°); C6–H6 ··· O1: 2.53 Å (152.6°)] are drawn as dotted lines. The sidewise π–π contacts (C10 ··· N2: 3.58 Å; C13 ··· N2: 3.64 Å) originated from the CH ··· N hydrogen bonds are omitted for clarity. N and O atoms are lightly shaded.

In crystals **3**–**9**, four co-planar adjacent host molecules self-assemble[5] to aggregate as two pairs (each of the two confronted molecules aggregated to form one pair) exclusively and create a flat sheet possessing circular cavities, as shown in Fig. 4. The electron-donating guest molecules have entirely planar structures and volumes allowing location within the cavities. The sheet consisting of co-planar host–guest aggregations stacks *antiprismatically* with an *offset* style to form the gold-like metal-lustrous inclusion crystals **3**–**9**. It is noteworthy that the stacking in **3**–**9** is not the *prismatic* (eclipsed) type that is necessary for the formation of a structure possessing straight channels.[6] This packing motif has been observed not only in the crystal structures of inclusion compounds **3**, **4** and **5**, but also in **7**, **8** and **9**. As a typical example, we describe here the crystal structure of the *p*-dimethoxybenzene inclusion crystal **8**. Fig. 5 shows the sheet-like structure of crystal **8**. The *p*-dimethoxybenzene guest exists in the host couples-encircled cavities running parallel to *bc* plane, and no effects of the guest's disorder[7] were observed because of its perfect C_2 symmetry. A closed circular network of π-systems is produced by the CH/N type hydrogen bonds[8] between the cyano nitrogen and the olefinic hydrogen atom of the host molecules [C10–H10 ··· N2: 2.65 Å (163.7°); C13–H13 ··· N2: 2.69 Å (171.3°)][8a,8d,9] and the short π–π contacts (C10 ··· N2: 3.58 Å; C13 ··· N2: 3.64 Å) originated from such CH/N type H bonds,[1–3] along with the CN ··· CN contacts (N1 ··· C28: 3.57 Å; N6 ··· C1: 3.59 Å). The sidewise π–π contacts (CN ··· C=C), which are found to commonly exist in this kind of material, are suggested to be responsible for the gold-like metallic lustre[1] Moreover, the host and the *p*-dimethoxybenzene guest interact with each other through a remarkably stronger C–H (host) ··· O (guest) hydrogen bond[8a,8c,10] [C6–H6 ··· O1: 2.53 Å (152.6°)] since the oxygen atom O1 in *p*-dimethoxybenzene guest works as an appropriate proton acceptor.[8a,11] The stronger C–H (host) ··· O (guest) interaction is surmised as a predominant factor stabilizing the inclusion crystal.[8c,12] In contrast, there are no remarkable host–guest hydrogen bonds and other interactions between the host and the relatively smaller *p*-xylene guest within the crystal lattice of **4** (Fig. 6).

Since the inclusion of a relatively large aromatic guest such as indene also occurs, and the consequent co-crystal is isostructural with the others, we surmised that aromatic molecules having a similar size to indene, such as naphthalene or benzo-

---

† CCDC reference numbers 205806–205811. See http://www.rsc.org/suppdata/ob/b3/b302689b/ for crystallographic data in .cif or other electronic format.

Table 1 Crystallographic data and structure refinement parameters

Inclusion compound	**3**	**4**	**5**	**6**	**7**	**8**
Empirical formula	$2C_{28}H_{11}N_7S_2{\cdot}C_7H_8$	$2C_{28}H_{11}N_7S_2{\cdot}C_8H_{10}$	$2C_{28}H_{11}N_7S_2{\cdot}C_7H_8O$	$2C_{28}H_{11}N_7S_2{\cdot}C_8H_{10}O_2$	$2C_{28}H_{11}N_7S_2{\cdot}C_8H_{10}O_2$	$2C_{28}H_{11}N_7S_2{\cdot}C_9H_8$
M_w	1111.29	1125.31	1127.29	1157.31	1157.31	1135.31
Crystal system	Monoclinic	Monoclinic	Monoclinic	Monoclinic	Monoclinic	Monoclinic
Space group	$P2_1/c$	$P2_1/c$	$P2_1/c$	$P2_1/\mathrm{c}$	$P2_1/\mathrm{c}$	$P2_1/\mathrm{c}$
Z	2	2	2	4	2	2
Cell constants						
a/Å	10.031 (2)	9.935 (3)	9.979 (3)	12.380 (7)	9.829 (5)	10.168 (6)
b/Å	27.595 (6)	27.547 (10)	27.550 (6)	27.61 (2)	27.691 (10)	27.708 (12)
c/Å	11.908 (5)	12.211 (6)	12.035 (5)	12.380 (5)	12.488 (7)	11.785 (11)
α/deg	90	90	90	90	90	90
β/deg	124.13 (5)	124.39 (5)	124.31 (5)	93.22 (5)	125.32 (6)	124.03 (9)
γ/deg	90	90	90	90	90	90
V/Å^3	2728 (2)	2740 (2)	2733 (2)	5575 (6)	2773 (2)	2752 (3)
μ/cm^{-1}	2.07	2.05	2.07	2.06	2.07	2.05
Crystal size/mm	0.35 × 0.15 × 0.15	0.40 × 0.25 × 0.15	0.50 × 0.40 × 0.35	0.50 × 0.40 × 0.35	0.50 × 0.20 × 0.15	0.55 × 0.45 × 0.40
D_{calc}/g cm^{-3}	1.353	1.364	1.370	1.379	1.386	1.370
T/K	298	298	298	298	298	298
Index ranges	$0 \leqq h \leqq 12$	$-12 \leqq h \leqq 12$	$-12 \leqq h \leqq 11$	$-15 \leqq h \leqq 15$	$0 \leqq h \leqq 11$	$0 \leqq h \leqq 12$
	$-33 \leqq k \leqq 0$	$-33 \leqq k \leqq 0$	$-33 \leqq k \leqq 0$	$-33 \leqq k \leqq 0$	$-32 \leqq k \leqq 0$	$0 \leqq k \leqq 33$
	$-14 \leqq l \leqq 12$	$-15 \leqq l \leqq 12$	$-14 \leqq l \leqq 11$	$0 \leqq l \leqq 19$	$-14 \leqq l \leqq 11$	$-14 \leqq l \leqq 12$
Reflns measured	5626	10612	5604	11716	5012	5659
Unique reflexions	5615	5514	5483	11216	4904	5488
Observed reflexions	3549	3076	3870	6378	3385	4023
Parameters	350	370	367	769	379	354
R_{int}	0.013	0.078	0.013	0.046	0.022	0.021
Criteria of I	3.00	3.00	3.00	3.00	3.00	3.00
GOOF	1.022	1.018	1.007	1.040	1.003	1.006
$R1$[a] (obsd data, $I > 3\sigma(I)$)	0.055	0.066	0.044	0.057	0.049	0.071
$wR2$[b] (all data, F^2 refinement)	0.087	0.090	0.070	0.088	0.062	0.271
Final difference peaks/eÅ^{-3}	−0.50, 0.99	−0.64, 0.51	−0.31, 0.51	−0.56, 0.55	−0.34, 0.35	−0.69, 1.04

[a] $R1 = \Sigma\{|F_0| - |F_c|\}/\Sigma|F_0|$. [b] $wR2 = [\Sigma w(F_0^2 - F_c^2)^2/\Sigma w(F_0^2)^2]^{1/2}$.

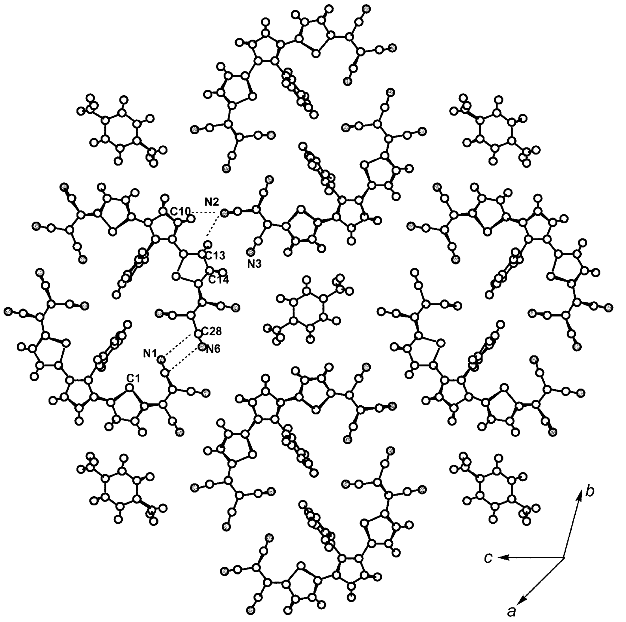

Fig. 6 Packing diagram of inclusion crystal **4** viewed along the *a*-axis. The CN ··· CN contacts (N1 ··· C28: 3.47 Å; N6 ··· C1: 3.54 Å) and the CH/N type hydrogen bonds [C10–H10 ··· N2: 2.60 Å (177.7°); C13–H13 ··· N2: 2.62 Å (172.3°)] are drawn as dotted lines. The sidewise π–π contacts (C10 ··· N2: 3.56 Å; C13 ··· N2: 3.57 Å; C14 ··· N3: 3.53 Å) originated from the CH ··· N hydrogen bonds are omitted for clarity. N atoms are lightly shaded.

thiophene, should also possibly display the same inclusion behavior. However, both naphthalene or benzothiophene failed to give crystalline inclusion.

Thermal gravimetry (TG) and differential scanning calorimetry (DSC) traces for the inclusion compounds **3**–**9** are shown in Fig. 7. All the inclusion crystals decompose in a single step in the weight loss curves, and the DSC traces show the first endotherm, due to guest release, followed by a sharp endotherm within the narrow range of 316–317 °C due to the melt of the host.

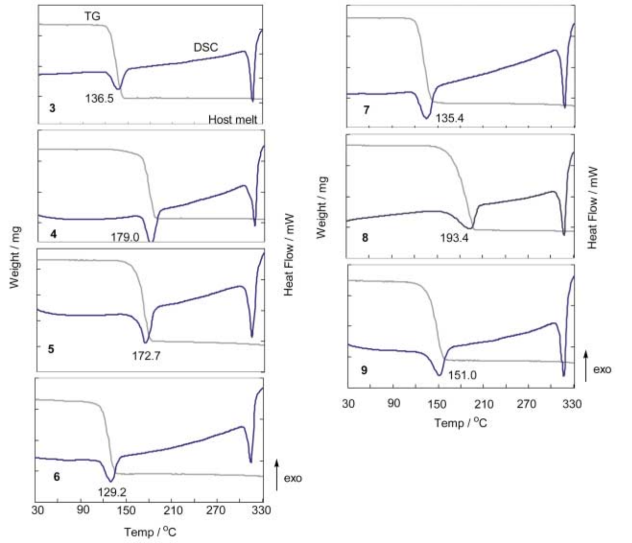

Fig. 7 Thermograms (TG and DSC) of the inclusion compounds **3**–**9**. The crystal number is represented with bold Arabic numerals.

The weight loss data of the inclusion compounds **3**–**9** derived from the TG traces are almost in agreement with the stoichiometric ratios of 2 : 1 (host/guest) obtained from ^{1}H NMR integration and X-ray diffraction. By comparing the DSC data of the dimethoxybenzene isomers included analogues, we suggest that inclusion compound containing C_2 symmetric guest shows higher thermal stability.

Conclusion

As stated above, attachment of two powerful electron-withdrawing tricyanoethenyl groups to 1-phenyl-2,5-di(2-thienyl)-pyrrole skeleton leads to a new versatile construction element which proved useful in crystalline inclusion and π-conjugated compound supramolecular chemistry. In inclusion compounds **3**–**9**, the host molecules self-assemble to aggregate as molecular pairs creating a flat sheet possessing circular cavities within which the aromatic guests are accommodated. The inclusion crystals show gold-like metallic lustre, suggesting that the origination of the metallic lustre is not exclusively limited to the tricyanoethenyl derivative itself, but possibly also to the crystalline inclusion compound containing tricyanoethenyl derivative. Based on the structural features of the inclusion crystals, we prefer to interpret the essential origin of the gold-like metallic lustre as due to the co-planar sheet-like crystal arrangement being extremely favorable to the sidewise intermolecular π–π contact (CN ··· C=C) between the host molecules. The DSC data of the analogs **3**–**9** proves that the C_2 symmetry of the guest molecules deeply influences their thermal stability. It is also noteworthy that the aromatic guest molecules suitable for the crystalline inclusion are all electron-donating. Combined with the fact that the electron-deficient quinone and 2,3-dichloro-5,6-dicyano-1,4-benzoquinone (DDQ) molecule cannot be included, we can infer that electrostatic forces also play a role in these supramolecular architectures.

Experimental

General

All chemicals were obtained from commercial suppliers and used without further purification. ^{1}H NMR spectra were recorded at 300 MHz using a Varian Gemini-2000 NMR spectrometer and chemical shifts were referenced to TMS as internal standard. Chemical shifts (δ_H) are quoted in parts per million (ppm). Coupling constants are quoted in Hertz (Hz). Thermal analyses (TG-DSC) were carried out on a Mac Science TG-DSC2000s apparatus. The measurements were performed over the temperature range 30–330 °C at a heating rate of 10 °C min^{-1} with a purge of dry nitrogen flowing at the pressure of *ca.* 0.15 MPa. UV-Vis absorption spectra in THF solution were recorded on a JASCO V-570 spectrophotometer at concentration of 3×10^{-5} mol l^{-1}. Solid-state UV-Vis-NIR diffuse reflection–absorption spectra were recorded on a JASCO V-570 spectrophotometer equipped with an integral detector. Single crystals of the corresponding compounds were uniformly broken into powder and were put into a quartz glass cell for measurement under the absorption response mode. Infrared spectra were measured on a JASCO FT/IR-350 spectrophotometer. Melting points are uncorrected. Elemental analyses were performed by Chemical Analysis Center of Chiba University. All X-ray powder diffraction (XRPD) analyses were taken on a Mac Science MXP powder diffractometer using graphite-monochromated Cu–Kα radiation (40 kV, 300 mA). The spectra were measured between 2° and 50° in the $2\theta/\theta$-scan mode with steps of 0.01° in 2θ and 4°min^{-1}.

Materials

Synthesis of the host compound. *1-Phenyl-2,5-bis[5-(tricyanoethenyl)-2-thienyl]pyrrole* **2**. A mixture of 1-phenyl-2,5-di(2-thienyl)pyrrole[1,4] (283 mg, 0.92 mmol) and TCNE (470 mg; 3.69 mmol) in 20 mL of anhydrous DMF was stirred for 24 h at 80 °C. The reaction mixture was cooled to room temperature, then the precipitated golden-yellow solid was separated by filtration (*ca.* 453 mg, 78% based upon pure **2**). The solid was washed with acetone (5 mL × 3) and then dried *in vacuo* at 80–100 °C until the colour changed to green. The filtrate was poured into a saturated NaCl solution, and the aqueous layer was extracted with toluene (20 mL × 6). The combined organic layer was dried over anhydrous $MgSO_4$ and concentrated *in vacuo*. The dark blue residue was purified by column chromatography (silica gel, $CHCl_3$) to afford the remaining portion as dark green powder (75 mg, 16%; total: 94%): mp 316.5–317.0 °C (Found: C, 65.82; H, 2.06; N, 19.27. Calc. for $C_{28}H_{11}N_7S_2$: C, 66.00; H, 2.18; N, 19.24%); ν_{max} (KBr)/cm^{-1} 2218 (CN), 1502, 1406, 1379, 1358, 1200, 1120, 778 and 696; λ_{max}/nm (ε/dm^3 mol^{-1} cm^{-1}) 644 (63300); δ_H ($CDCl_3$) 7.09 (2 H, d, *J* 4.5, thiophene-3-CH=CH), 7.11 (2 H, s, pyrrole-CH=CH), 7.47 (2 H, d, *J* 8.7, Ar), 7.71 (2 H, t, *J* 8.0, Ar), 7.80 (1 H, t, *J* 7.4, Ar) and 7.82 (2 H, d, *J* 4.5, thiophene-4-CH=CH).

Preparation of single crystals of the crystalline inclusion compounds. The inclusion compounds **3**, **4** and **5** were obtained by dissolving the host compound **2** into the minimum amount of guest. The corresponding single crystals appeared by slow evaporation at ambient temperature. The inclusion compounds **6**–**9** were prepared by dissolving the corresponding host–guest mixture (H/G = 1 : 3 or 1 : 4) into the minimum amount of $CHCl_3$ solvent. The corresponding single crystals grew by slow evaporation of $CHCl_3$ at room temperature. The inclusion compounds **5**, **6**, **7** and **9** could also be formed slow diffusion of hexane into the corresponding guest solution of the host **2**. However, this method was not effective enough to get single crystals for X-ray structural analysis.

Inclusion compounds

3. Gold-like lustrous crystals: dec (TG-DSC) 136.5 °C (Found: C, 67.86; H, 2.78; N, 17.48. Calc. for $2C_{28}H_{11}N_7S_2\cdot C_7H_8$: C, 68.09; H, 2.72; N, 17.65%).

4. Gold-like lustrous crystals: dec (TG-DSC) 179.0 °C (Found: C, 68.29; H, 2.88; N, 17.17. Calc. for $2C_{28}H_{11}N_7S_2\cdot C_8H_{10}$: C, 68.31; H, 2.87; N, 17.43%).

5. Gold-like lustrous crystals: dec (TG-DSC) 172.7 °C (Found: C, 67.13; H, 2.83; N, 17.18. Calc. for $2C_{28}H_{11}N_7S_2\cdot C_7H_8O$: C, 67.13; H, 2.68; N, 17.40%).

6. Gold-like lustrous crystals; dec (TG-DSC) 129.2 °C (Found: C, 66.08; H, 2.84; N, 16.68. Calc. for $2C_{28}H_{11}N_7S_2\cdot C_8H_{10}O_2$: C, 66.42; H, 2.79; N, 16.94%).

7. Gold-like lustrous crystals; dec (TG-DSC) 135.4 °C (Found: C, 66.48; H, 2.88; N, 16.59. Calc. for $2C_{28}H_{11}N_7S_2\cdot C_8H_{10}O_2$: C, 66.42; H, 2.79; N, 16.94%).

8. Gold-like lustrous crystals; dec (TG-DSC) 193.4 °C (Found: C, 66.19; H, 2.71; N, 16.86. Calc. for $2C_{28}H_{11}N_7S_2\cdot C_8H_{10}O_2$: C, 66.42; H, 2.79; N, 16.94%).

9. Gold-like lustrous crystals; dec (TG-DSC) 151.0 °C (Found: C, 68.71; H, 2.64; N, 17.19. Calc. for $2C_{28}H_{11}N_7S_2\cdot C_9H_8$: C, 68.77; H, 2.66; N, 17.27%).

X-Ray crystallography

Data collections were performed on a Mac Science MXC18 four-circle diffractometer with graphite monochromated Cu–Kα radiation (λ = 1.54178 Å) using the ω-2θ scan technique at 298 K. The structures were solved by direct methods and refined by full-matrix least-squares methods against F^2 (SIR 92[13] on a computer program package; maXus ver. 4.3p2 Bruker-AXS). For compounds, **4**, **7**, and **8**, all non-hydrogen atoms were refined with anisotropic displacement parameters and hydrogen atoms were refined isotropically. In compounds, **3**, **5**, and **9**, heavy atoms were refined anisotropically except for those of the guest molecule. No empirical absorption correction was applied to all crystal refinements. For compound **5**, the guest (anisole) is disordered over 2 sites but the occupancies for each atom are not the same as each other, and have a wide range of values.

Acknowledgements

This work was supported by a Grant-in-Aid for Scientific Research (No. 14350464) from the Ministry of Education, Culture, Sports, Science, and Technology of Japan.

References and notes

1 K. Ogura, R. Zhao, H. Yanai, K. Maeda, R. Tozawa, S. Matsumoto and M. Akazome, *Bull. Chem. Soc. Jpn.*, 2002, **75**, 2359.

2 R. Zhao, M. Akazome, S. Matsumoto and K. Ogura, *Tetrahedron*, 2002, **58**, 10225.

3 R. Zhao, S. Matsumoto, M. Akazome and K. Ogura, *Tetrahedron*, 2002, **58**, 10233.

4 K. Ogura, H. Yanai, M. Miokawa and M. Akazome, *Tetrahedron Lett.*, 1999, **40**, 8887.

5 For the newest information, trends and prospects in self-assemble, see: (*a*) J.-M. Lehn, *Science*, 2002, **295**, 2400; (*b*) O. Ikkata and G. ten Brinke, *Science*, 2002, **295**, 2407; (*c*) T. Kato, *Science*, 2002, **295**, 2414; (*d*) G. M. Whitesides and B. Brzybowski, *Science*, 2002, **295**, 2418. See also; (*e*) D. Philp and J. F. Stoddart, *Angew. Chem., Int. Ed. Engl.*, 1996, **35**, 1154; (*f*) C. A. Hunter, *Angew. Chem., Int. Ed. Engl.*, 1995, **34**, 1079; (*g*) D. S. Lawrence, T. Jiang and M. Levett, *Chem. Rev.*, 1995, **95**, 2229; (*h*) F. M. Menger, S. S. Lee and X. Tao, *Adv. Mater.*, 1995, **7**, 669; (*i*) M. R. Ghadiri, *Adv. Mater.*, 1995, **7**, 675.

6 (*a*) M. J. Horner, K. T. Holman and M. D. Ward, *Angew. Chem., Int. Ed.*, 2001, **40**, 4045; (*b*) M. Akazome, Y. Ueno, H. Ooiso and K. Ogura, *J. Org. Chem.*, 2000, **65**, 68; (*c*) M. Akazome, M. Noguchi, O. Tanaka, A. Sumikawa, T. Uchida and K. Ogura, *Tetrahedron*, 1997, **53**, 8315; (*d*) K. Ogura, T. Uchida, M. Noguchi, M. Minoguchi, A. Murata, M. Fujita and K. Ogata, *Tetrahedron lett.*, 1990, **31**, 3331; (*e*) M. Akazome, Y. Yanagita, R. Sonobe and K. Ogura, *Bull. Chem. Soc. Jpn.*, 1997, **70**, 2823.

7 In crystals **3** and **5**, disordered guests with two crystallographically equivalent alternative conformations were observed because of the asymmetry of the substituent on their central *N*-phenyl ring.

8 Some information and examples on CH/N type hydrogen-bonding interactions, see: (*a*) M. Hartmann, D. S. Wetmore and L. Radom, *J. Phys. Chem. A*, 2001, **105**, 4470; (*b*) R. Taylor and O. Kennard, *J. Am. Chem. Soc.*, 1982, **104**, 5063; (*c*) P. Seiler and J. D. Dunitz, *Helv. Chim. Acta*, 1989, **72**, 1125; (*d*) K. N. Houk, S. Menzer, S. P. Newton, F. M. Raymo, J. F. Stoddart and D. J. Williams, *J. Am. Chem. Soc.*, 1999, **121**, 1479; (*e*) Y. E. Ovchinnikov, O. V. Shishkin, Y. T. Struchkov and G. R. Desiraju, *J. Am. Chem. Soc.*, 1996, **118**, 4085; . See also: K. Sato, S. Arai and T. Yamagishi, *Tetrahedron Lett.*, 1999, **40**, 5219 and the references therein.

9 For examples on [C–H ··· N] hydrogen-bonding interactions, see: (*a*) T. Fukushima, N. Okazeri, T. Miyashi, K. Suzuki, Y. Yamashita and T. Suzuki, *Tetrahedron Lett.*, 1999, **40**, 1175; (*b*) D. S. Reddy, B. S. Goud, K. Panneerselvam and G. R. Desiraju, *J. Chem. Soc., Chem. Commun.*, 1993, 663; (*c*) M. Mazik, D. Bläser and R. Boese, *Tetrahedron Lett.*, 2000, **41**, 5827; (*d*) G. R. Desiraju, *Angew. Chem., Int. Ed. Engl.*, 1995, **34**, 2311; (*e*) P. N. Jagg, P. F. Kelly, H. S. Rzepa, D. J. Williams, J. D. Woollins and W. Wylie, *J. Chem. Soc., Chem. Commun.*, 1991, 942; (*f*) F. A. Cotton, L. M. Daniels, G. T. Jordan and C. A. Murillo, *Chem. Commun.*, 1997, 1673; (*g*) J. Ashmore, R. Bishop, D. C. Craig and M. L. Scudder, *Cryst. Eng. Comm.*, 2002, **4**, 194.

10 For examples on [C–H ··· O] hydrogen-bonding interactions, see: (*a*) D. J. Sutor, *Nature*, 1962, **195**, 68; (*b*) M. Sandaralingam, *Nature*, 1966, **217**, 35; (*c*) J. A. R. P. Sarma and G. R. Desiraju, *J. Chem. Soc., Perkin Trans. 2*, 1987, 1195; (*d*) G. R. Desiraju, *J. Chem. Soc., Chem. Commun.*, 1989, 179; (*e*) T. Steiner and G. R. Desiraju, *Chem. Commun.*, 1998, 891; (*f*) G. R. Desiraju, *Acc. Chem. Res.*, 1991, **24**, 290; (*g*) G. R. Desiraju, *Acc. Chem. Res.*, 1996, **29**, 441; (*h*) C. V. K. Sharma and M. J. Zaworotko, *Chem. Commun.*, 1996, 2655; (*i*) T. Steiner, *Chem. Commun.*, 1997, 727; (*j*) S. G. Bodige, R. D. Rogers and S. C. Blackstock, *Chem. Commun.*, 1997, 1669; (*k*) I. Berger and M. Egli, *Chem. Eur. J.*, 1997, **3**, 1400; (*l*) Y.-L. Gu, T. Kar and S. Scheiner, *J. Am. Chem. Soc.*, 1999, **121**, 9411.

11 S. Apel, S. Nitsche, K. Beketov, W. Seichter, J. Seidel and E. Weber, *J. Chem. Soc., Perkin Trans. 2*, 2001, 1212.

12 (*a*) M. Asakawa, C. L. Brown, S. Menzer, F. M. Raymo, J. F. Stoddart and D. J. Williams, *J. Am. Chem. Soc.*, 1997, **119**, 2614; (*b*) P. L. Anelli, P. R. Ashton, R. Ballardini, V. Balzani, M. Delgado, M. T. Gandolfi, T. T. Goodnow, A. E. Kaifer, D. Philp, M. Pietraszkiewicz, L. Prodi, M. V. Reddington, A. M. Z. Slawin, N. Spencer, J. F. Stoddart, C. Vicent and D. J. Williams, *J. Am. Chem. Soc.*, 1992, **114**, 193.; See also: S. Tsuzuki, H. Houjou, Y. Nagawa and K. Hiratani, *J. Chem. Soc., Perkin Trans. 2*, 2002, 1271.

13 A. Altomare, G. Cascarano, C. Giacovazzo, A. Guagliardi, M. C. Burla, G. Polidori and M. Camalli, *J. Appl. Cryst.*, 1994, **27**, 435.